Available online at www.sciencedirect.com
ScienceDirect
Journal of the European Ceramic Society 31 (2011) 1491–1496
www.elsevier.com/locate/jeurceramsoc

Mechanochemically activated synthesis of zirconium carbide nanoparticles at room temperature: A simple route to prepare nanoparticles of transition metal carbides

J.Y. Xiang [a], S.C. Liu [a], W.T. Hu [a], Y. Zhang [a], C.K. Chen [a], P. Wang [a], J.L. He [a], D.L. Yu [a], B. Xu [a], Y.F. Lu [b], Y.J. Tian [a], Z.Y. Liu [a,*]

[a] *State Key Laboratory for Metastable Materials Science and Technology, Yanshan University, Qinhuangdao 066004, China*
[b] *Northwest Institute for Nonferrous Metal Research, P.O. Box 51, Xi'an, Shaanxi 710016, China*

Received 31 August 2010; received in revised form 9 January 2011; accepted 25 January 2011
Available online 18 February 2011

Abstract

Mechanically activated syntheses of zirconium carbides (ZrC_x) nanoparticles have been performed via ball milling of Zr powder with toluene. It has been found that the milling time can be used to tune the ratio x of C to Zr. The spark plasma sintering of the ZrC_x nanoparticles has shown that the densification can be achieved at a considerably reduced temperature of 1200 °C. This ball milling procedure has been tried to successfully synthesize the nanoparticles of WC_x, TiC_x, and NbC_x, demonstrating that it is a potential route to prepare the nanoparticles of transition metal carbides.

Keywords: Milling; Grain size; Spark plasma sintering; Carbides; Solid liquid reaction

1. Introduction

Zirconium carbide of ZrC_x is a nonstoichiometric compound with the fcc NaCl crystal structure, and the ratio of C to Zr can be varied from 0.3 to 0.98.[1,2] Due to the mixture of ionic, covalent, and metallic bonding, ZrC_x presents excellent physical and chemical properties such as high melting temperatures (maximized at 3420 °C and $ZrC_{0.82}$[3]), high hardness (maximized at ~25.8 GPa and $ZrC_{0.96}$[1,4,5]), high thermal and electrical conductivity,[6] and high chemical stability.[1,7] Thus, ZrC_x is a promising material for applications in cutting tools, high-speed aircraft leading edges[8] operating in high or ultra-high temperature, the thermal-field emitters,[9] etc. ZrC_x is also an important material for nuclear reactor core owing to its low neutron cross-section.[10]

Fabrications of ZrC_x have been reported by the reactions of zirconium, zirconium hydrides (ZrH_2), and zirconium dioxides (ZrO_2) with carbon.[6,11–13] Owing to the difficulty of mixing the reactants on a fine scale (e.g., molecular-scale mixing), these synthesizing processes generally require relatively high reaction temperature and long soaking time of several hours or more. The high synthesizing temperature usually leads to the fast growth of the ZrC_x grains, making it difficult to obtain the ZrC_x products with grains in nano or ultrafine scales. To sinter the highly dense bulk transition-metal carbides with desirable microstructural features, the first and perhaps the most important step is the preparation of fine and homogeneous nanoparticles as precursor. Mechanochemical synthesis or mechanical alloying is a potential synthesizing process for nanoparticles of the transition-metal carbides without external heat source.[14,15] There are reports for the formation of ZrC_x nanoparticles by mechanically milling of Zr or ZrO_2 with carbon.[16,17] Generally, cold-welding is hard to be avoided in the process of directly milling Zr with carbon,[18] which makes it difficult to obtain the ZrC_x nanoparticles with a uniform distribution of size. In the mechanically milling process, process control agents (PCAs) can be used to avoid cold-welding and improve the pulverization of the materials.[19] In comparison with solid PCAs, organic solutions have been widely chosen as PCA since they can fast cover the exposed fresh surface of milled particle, and easy to be removed from the final products.

* Corresponding author.
E-mail address: liuzy0319@yahoo.com (Z.Y. Liu).

0955-2219/$ – see front matter © 2011 Elsevier Ltd. All rights reserved.
doi:10.1016/j.jeurceramsoc.2011.01.022

On one hand, PCAs have to be both thermally and chemically stable during ball milling in order to obtain materials with refined grains and minimized contaminants. On the other hand, it has been reported that some organic additives are likely to be decomposed during the process of high-energy ball milling, forming fine dispersions of metal carbides such as Fe_3C,[20,21] Al_4C_3,[22,23] TiC,[22,24] and NbC[25] in the metals or metal alloys. Formation of NbC powder was reported during the grinding of Nb and graphite powder mixture with hexane or methanol, and was considered to the mechanically assisted reaction of carbon with the intermediate product of NbH_x.[26] By mechanochemically milling metal powders with different organic substances, powders of metal carbides (such as Fe_3C[27]), metal nitrides (such as AlN,[28] TiN,[29,30] and Fe_3N[31,32]), and metal hydrides (such as TiH_x,[33] ZrH_x,[34] and NbH_x[26,35]) had been reported to be synthesized. Suzuki and coworkers reported the formation of phases with fcc-like structure resembling that of ZrC or TiC during the milling of Zr powder or Ti powder with n-heptane.[36,37] Presumably, the observed fcc phases were hydrides of Zr or Ti, since these metastable compounds changed to original hcp structure upon heating.[36,37] So far it is not clear of the mechanism for the formation of metal carbides, nitrides, and hydrides during the mechanochemically milling with organic media. It seems that by intentionally choosing an instable PCA for the ball milling, it decomposes and releases atomic carbon, hydrogen, and/or nitrogen, providing highly reactive agents for the preparation of highly pure metal hydrides, carbides, and/or nitrides with a considerably small grain size.

In this article, we present a method to prepare zirconium carbide nanopowder by mechanochemically milling of the Zr powder with toluene, indicate a potential simple route for synthesis of nanopowders of carbides of transition metals such as Zr, Ti, W, and Nb by milling them with toluene.

2. Experimental procedure

In the present work, detailed investigations have been performed on the preparations of ZrC_x nanoparticles by ball milling of Zr powder (−325 mesh, purity 99.5%) in toluene using a planetary ball mill (P4, Fritsch, Germany). Tungsten carbide vials and balls were used. The weight ratio of ball to Zr powder was chosen to be 13:1, and that of toluene to Zr powder was 3:1. The Zr powder and toluene were introduced in a WC vial and sealed in a glove box filled with highly pure argon gas. The rotation speed during milling was set to be 400 rpm. The collected products after milling were in a mash state, and they were dried at 80 °C for 20 h in a vacuum chamber ($\sim 10^{-3}$ Pa) to remove any residue of toluene. The structural development of the as-milled powders was characterized by X-ray diffraction (XRD) (Cu Kα radiation, D/MAX-PC/2500), field-emission scan electron microscopy (SEM S4800, equipped with an energy-dispersive X-ray compositional microanalysis system, EDS), high resolution transmission electron microscopy (HRTEM JEOL 2010). Bulk ZrC_x was sintered at 1200 °C under pressure of 50 MPa for 5 min using a spark plasma sintering (SPS) system (Syntex Inc., Japan). Average grain size was determined from the peak broadening using the Williamson–Hall formula[38] after elimination of the respective influence of strain and instrumental broadening by a pseudo-Voigt profile function fitting and comparing the relevant peaks with that from a standard sample SPS-sintered at 2000 °C and 20 MPa for 1 h and slow cooled down to room temperature. Carbon content for the samples was analyzed by oxidation. The density was measured using an Archimedes method. The Vickers indentation was obtained by indenting a diamond indenter into the samples with 300 g loads applied for 10 s.

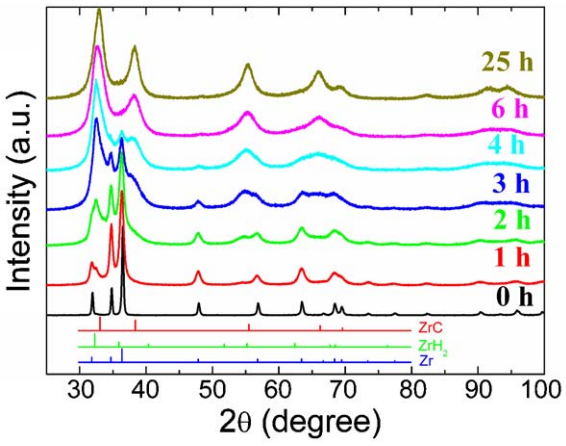

Fig. 1. Typical XRD patterns of as-supplied Zr powder and as-milled powders obtained after different milling times. The bars, from top to bottom, are corresponding to ZrC (red, PDF#74-1221), ZrH_2 (green, PDF#73-2067), and Zr (blue, PDF#05-0665), respectively. (For interpretation of the references to color in this figure legend, the reader is referred to the web version of this article.)

3. Results and discussion

Fig. 1 shows the X-ray diffraction (XRD) patterns of the as-supplied Zr powder and the as-milled powders after the milling durations t of 1, 2, 3, 4, 6, and 25 h. With the increase of t, the diffraction peaks of the as-supplied hcp Zr were weakened and broadened quickly, becoming invisible when t is longer than 6 h. Accompanying the milling-induced disappearance of Zr, two more new phases were observed in the XRD spectra, and they were identified as fcc-ZrH_2 and fcc-ZrC_x. In the early milling stage of $t < 3$ h, the formation of ZrH_2 phase dominates. This is in an agreement with the formation of metal hydrides during the milling of metals with organic additives containing a hydrogen component.[26,34,35] When the milling duration increases above 1 h, the reflection peaks of ZrC_x were found to appear. They grew continuously in intensity with the increase of t, and become dominant when t is longer than 3 h. By analyses of the XRD spectra with the help of the MAUD programs,[39] the developments of Zr, ZrH_2, and ZrC_x phases with the milling time have been determined in volume fraction and grain size,[40] which are shown in Fig. 2. Sharp reductions in the volume fraction and grain size occur for the Zr phase in the early milling stage ($t < 1$ h). The Zr grains go quickly towards an average size in nanoscale (less than 10 nm) when $t > 1$ h, and the Zr phase cannot be detected in the XRD measurements at $t > 6$ h. With the increase of milling time t, the formation of ZrH_2 dominates in the early milling stage, reach-

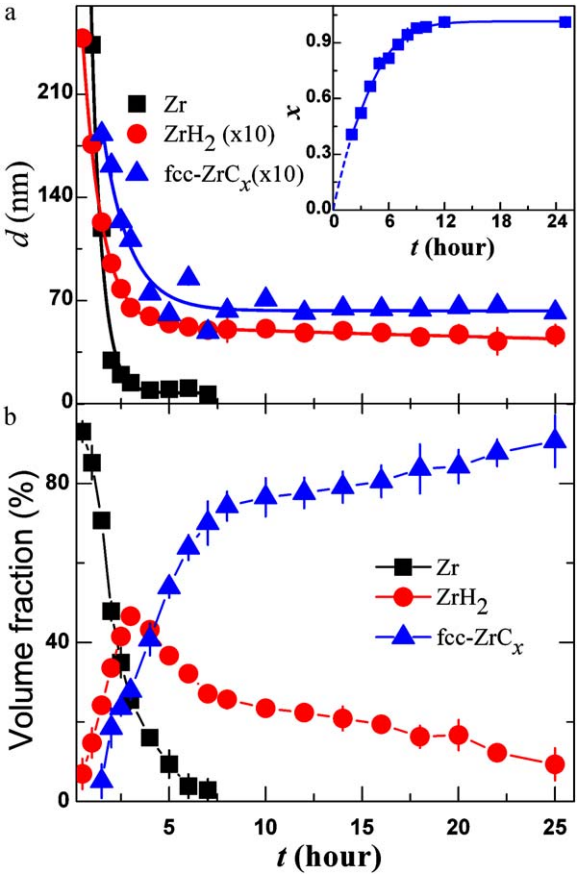

Fig. 2. Developments of the average grain size d (a) and volume fraction (b) for Zr, ZrH_2, and ZrC_x with the milling duration t. For clearance, the grain sizes for ZrH_2 and ZrC_x were enlarged by a factor of 10. Inset of (a) is the average carbon content of the as-milled powders after different milling times.

ing a maximum at the milling time of 3 h. At $t > 3$ h, the ZrH_2 phase disappears gradually. In contrast, the new ZrC_x phase is almost invisible in the early milling process, but when the milling time is longer than 1 h, its formation starts and grows rapidly with the milling time. For both the phases of ZrH_2 and ZrC_x, their average grain sizes were determined to be in nanoscale even in the early milling stage, and they were reduced quickly to a value of ~7 nm by the ball milling. When the milling is long enough, for instance, $t = 25$ h, the volume fraction of ZrC_x was estimated to be ~90%, indicating that the finally obtained nanoparticles after the milling consist mainly of the phase of ZrC_x.

Fig. 3 shows the TEM and HRTEM images of the nanoparticles obtained after the 25 h milling. The nanoparticles are fairly agglomerated, and the average size is determined to be less than 10 nm. This value is consistent with the average grain size (~7 nm) estimated from the XRD spectra. The HRTEM image indicates that the nanoparticles are single crystalline. In combination with the XRD patterns, the selected area electron diffraction (SAED) rings (lower right inset of Fig. 3) and the HRTEM image support the fcc structure of the nanoparticles. A previous report claimed that the milling of Zr in toluene can induce an allotropic transformation of Zr from hcp to fcc due to the reduced grain size of Zr.[41] However, our investigations

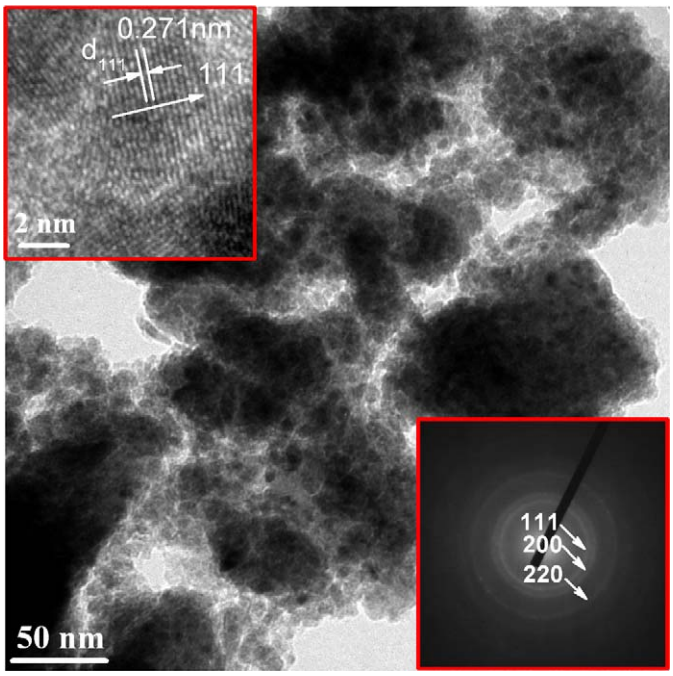

Fig. 3. TEM images of the as-milled powders after 25 h of milling. Upper and lower insets are the HRTEM image and the SAED rings, respectively.

have shown that the fcc phase is the nonstoichiometric ZrC_x. As shown in the inset of Fig. 2(a), the determined average carbon content was found to increase with the increase of t, converging to a value of 1 when the milling duration t is longer than $t > 10$ h.

Fig. 4(a) shows the XRD pattern for the SPS-sintered sample from the 25 h-milled nanoparticles. The reflection peaks are found to come from the fcc structure of ZrC (JSPDS-PDF #65-0962),[42] and the refined lattice constant is ~0.4698 nm. The C content x was determined to be 0.995, being consistent with that of the as-milled nanoparticles before sintering. In addition, the measured Vickers hardness for the SPS-sintered sample was found to be ~14 GPa, and it is much higher than the value (~2.1 GPa) found in the sintered starting Zr powder. These experimental facts corroborate that the nanoparticles obtained by the milling of Zr in toluene are the zirconium carbides of ZrC_x instead of the previously claimed fcc Zr.[41]

The SPS-sintered sample shows a high relative density of ~99.85%. The SEM images on the fracture surface (Fig. 4(b)) show that the grains have a narrow size distribution and are quite well connected. The average grain size is estimated to be ~5 μm from the SEM image. There are also particles seen on the grain boundary, as indicated by circles in the inset of Fig. 4(b), and they were identified to be W using the EDS compositional analysis. Since the W phase was not detected within the resolution of our XRD machine, such a small amount of W was presumably produced from the reaction of Zr with the tungsten carbide milling media.

During the liquid–solid reaction induced by ball milling of Zr in toluene, toluene serves as the carbon source for the formation of ZrC_x. The measurements of XRD and SEM indicate

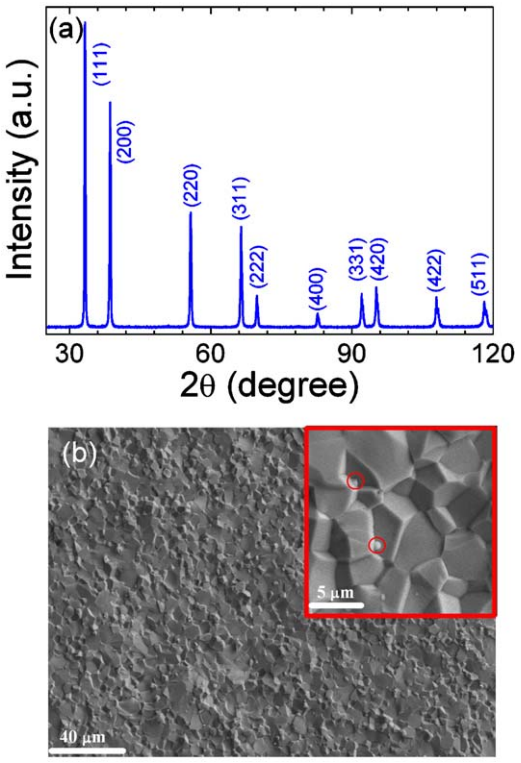

Fig. 4. (a) The XRD pattern for the SPS-sintered sample from the 25 h milled nanoparticles. Inset of (a) is the Raman spectra for the as-milled nanoparticles (red solid circles) and the SPS-sintered sample (blue solid squares). Solid lines are guide to the eyes. (b) SEM images of the fracture surface for the SPS-sintered sample at 1200 °C for 5 min. The inset of (b) is the enlarged SEM image, in which some W particles (red circles) are observed. (For interpretation of the references to color in this figure legend, the reader is referred to the web version of this article.)

that the reaction process activated by high-energy ball impact can be separated into three main stages. The first milling stage ($t < \sim 1$ h) is mainly dominated by the refinement of the Zr particles, in which toluene serves as a PCA for prevention of the Zr cold-welding. The formation of ZrH_2 dominates the second milling stage (1 h $< t <$ 4 h). When the Zr particles are decreased to a critical size (~50 nm), they may serve as a catalyst to the decomposition of toluene into carbon and hydrogen. The formation enthalpy of ZrH_2[43] is much lower than that of ZrC,[44] and the mobility of H in the Zr lattice is much higher than the C mobility. Thus, the formation of ZrH_2 under high-energy ball impact is favorable. The Zr particles are covered with quickly formed thin shells of nanocrystalline ZrH_2, preventing the further decomposition of toluene owing to the disappearance of fresh Zr surfaces. Simultaneously, the free C atoms tend to absorb on the ZrH_2 shells. This is confirmed by the XRD results, SEM morphology (Fig. 5(a)) and concentration profiles of elemental Zr and C of particles (Fig. 5(b)). The sharp reduction of Zr in concentration at the edge outwards to the hole, being gradually decreased further away the hole, is probably due to the formation of zirconium hydrides since the concentration of C remains barely changed over the particle. Under high-energy ball impacts, the brittle shells of ZrH_2 are broken and fall off the Zr particles, generating the new fresh Zr surfaces. The exposure of fresh Zr surface to toluene leads to the further decomposition of toluene, and thin shells of ZrH_2 are formed again around the Zr particles. This process also induces the quick size reduction of the Zr particles, and it repeats till Zr disappears almost completely. Accompanying the disappearance of Zr and the continuous formation of ZrH_2, the ZrC_x phase forms by the reaction between broken off ZrH_2 nanoparticles and liberated free C atoms under the high-energy ball pulverization. In fact, by the milling of ZrH_2 in toluene and ZrH_2 with graphite, we found that ZrC_x was produced only in the latter case. This is similar to the synthesis of ZrC_x by the ball milling of Zr and carbon under hydrogen atmosphere.[45] The final milling stage ($t > 4$ h) is dominated by the formation of ZrC_x via the reaction of broken ZrH_2 nanoparticles with liberated free C atoms, since Zr-C chemical bonds are more thermally stable than Zr-H bonds[46].

By similar procedures, nanoparticles of NbC_x, TiC_x, and WC_x were synthesized only with different ball milling times, which is 40 h, 50 h and 60 h, respectively for the starting powder of W, Ti, and Nb, as shown in Fig. 6. The corresponding average grain size d is ~8 nm, ~7 nm and ~8 nm, and atomic ratio of carbon to metal x is 0.657, 0.953 and 0.998, respectively for NbC_x, TiC_x and WC_x. These results indicate that the mechanochemically milling of the transition metals powder with toluene could be a potential route to synthesize the nanoparticles (~10 nm) of transition-metal carbides.

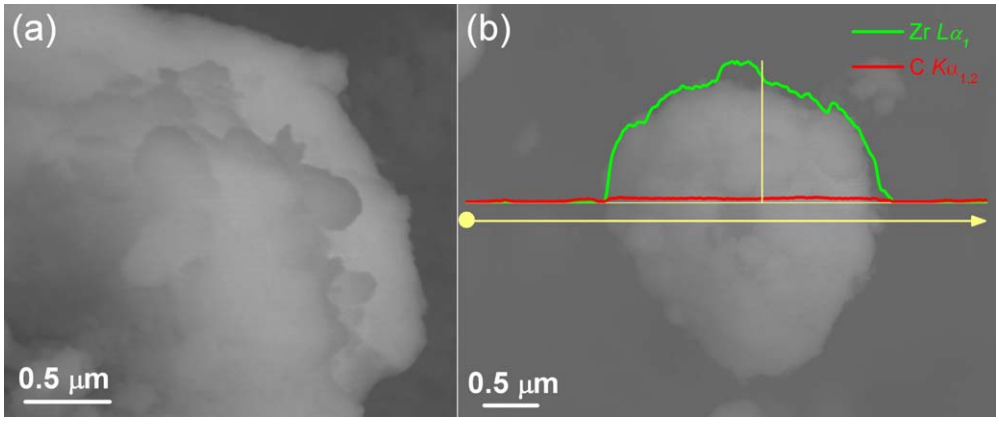

Fig. 5. (a) The SEM morphology and (b) the SEM line-scan image and the concentration profiles of elemental Zr and C, of particles obtained after 3 h of ball milling.

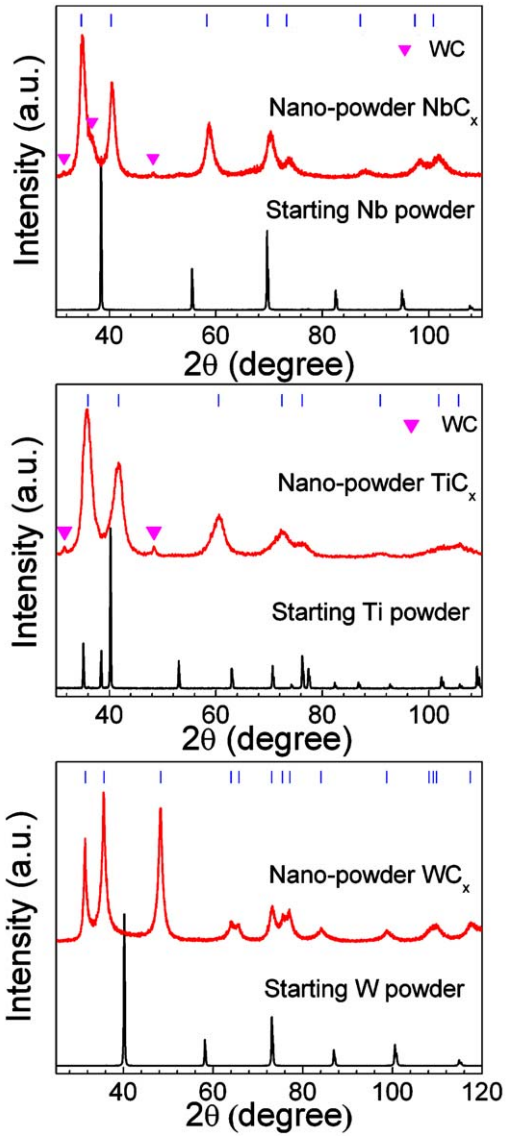

Fig. 6. XRD patterns for the as-supplied and as-milled powders of (a) Nb powder (particle size 44 μm, purity 98.5%), (b) Ti powder (particle size 74 μm, purity 99.5%), and (c) W powder (particle size 44 μm, purity 99.9%). The bars on the top of (a), (b), and (c) represent the positions for the diffraction peaks of NbC (PDF#38-1364), TiC (PDF#32-1383), and WC (PDF#51-0939), respectively.

4. Summary

In summary, nanoparticles of zirconium carbides were successfully produced by ball milling of Zr powder with toluene. During the milling, toluene served as a PCA as well as a source of carbon for the formation of ZrC_x. The carbon content of x can be tuned by controlling the ball milling time. Bulk ZrC from the SPS-sintering of the as-milled nanoparticles of ZrC_x at 1200 °C shows a Vickers hardness of ~14 GPa and relative density of ~99.8%. This ball milling process has been used to successfully prepare the nanoparticles of WC_x, TiC_x, and NbC_x, indicating that ball milling of the transition metals in toluene could be a potential route to synthesize the nanoparticles of transition-metal carbides.

Acknowledgements

Financial supports from the National Basic Research Program of China (Grant No. 2010CB731605, No. 50872118, and No. 58021001) and National Science Fund for Distinguished Young Scholars (Grant No. 51025103) are gratefully acknowledged.

References

1. Pierson HO. *Handbook of refractory carbides and nitrides—properties, characteristics, processing and applications*. New Mexico: Albuquerque; 1996.
2. Gusev AI. Order–disorder transformations and phase equilibrium in strongly nonstoichiometric compounds. *Physics—Uspekhi* 2000;**43**:1–37.
3. Sara RV. System zirconium–carbon. *J Am Ceram Soc* 1965;**48**:243–7.
4. Ramqvist L. Variation of lattice parameter and hardness with carbon content of group 4 b metal carbides. *Jernkontorets Annaler* 1968;**152**:517–23.
5. Samsonov GV, Naumenko VY, Okhremch Ln. Synthesis and properties of carbides of transition metals in their homogeneity range. *Phys Status Solidi A* 1971;**6**:201–11.
6. Toth LE. *Transition metal carbides and nitrides*. New York: Academic Press; 1971.
7. Oyama ST. *The chemistry of transition metal carbides and nitrides*. Glasgow: Blackie Academic & Professional; 1996.
8. Van Wie DM, Drewry DG, King DE, Hudson CM. The hypersonic environment: required operating conditions and design challenges. *J Mater Sci* 2004;**39**:5915–24.
9. Yada K, Masaoka H, Shoji Y, Tanji T. Studies of refractory carbides, nitrides, and borides as the thermionic emitters for electron-microscopy. *J Electron Microsc Tech* 1989;**12**:252–61.
10. Ogawa T, Ikawa K. Diffusion of metal fission-products in $ZrC_{1.0}$. *J Nucl Mater* 1982;**105**:331–4.
11. Berger LM, Gruner W, Langholf E, Stolle S. On the mechanism of carbothermal reduction processes of TiO_2 and ZrO_2. *Int J Refract Met Hard Mater* 1999;**17**:235–43.
12. Maitre A, Lefort P. Solid state reaction of zirconia with carbon. *Solid State Ionics* 1997;**104**:109–22.
13. Sarkar SK, Millerad, Mueller JI. Solubility of oxygen in ZrC. *J Am Ceram Soc* 1972;**55**:628–30.
14. Lin IJ, Nadiv S. Review of the phase-transformation and synthesis of inorganic solids obtained by mechanical treatment (mechanochemical reactions). *Mater Sci Eng* 1979;**39**:193–209.
15. Matteazzi P, LeCaër G, Mocellin A. Synthesis of nanostructured materials by mechanical alloying. *Ceram Int* 1997;**23**:39–44.
16. Matteazzi P, Lecaër G. Room-temperature mechanosynthesis of carbides by grinding of elemental powders. *J Am Ceram Soc* 1991;**74**:1382–90.
17. Takacs L. Ball milling-induced combustion in powder mixtures containing titanium, zirconium, or hafnium. *J Solid State Chem* 1996;**125**:75–84.
18. Gilman PS, Benjamin JS. Mechanical alloying. *Annu Rev Mater Sci* 1983;**13**:279–300.
19. Suryanarayana C, Ivanov E, Boldyrev VV. The science and technology of mechanical alloying. *Mater Sci Eng A* 2001;**304**:151–8.
20. Yelsukov EP, Lomayeva SF, Konygin GN, Dorofeev GA, Povstugar VI, Mikhailova SS, et al. Structure, phase composition and magnetic characteristics of the nanocrystalline iron obtained by mechanical milling in heptane. *Nanostruct Mater* 1999;**12**:483–6.
21. Lomayeva SF, Yelsukov EP, Konygin GN, Dorofeev GA, Povstugar VI, Mikhailova SS, et al. The influence of a surfactant on the characteristics of the iron powders obtained by mechanical milling in organic media. *Colloids Surf A: Physicochem Eng Aspects* 2000;**162**:279–84.
22. Singer RF, Oliver WC, Nix WD. Identification of dispersoid phases created in aluminum during mechanical alloying. *Metall Trans A—Phys Metall Mater Sci* 1980;**11**:1895–901.

23. Kleiner S, Bertocco F, Khalid FA, Beffort O. Decomposition of process control agent during mechanical milling and its influence on displacement reactions in the Al–TiO_2 system. *Mater Chem Phys* 2005;**89**:362–6.
24. Lee W, Kwun SI. The effects of process control agents on mechanical alloying mechanisms in the Ti–A1 system. *J Alloys Compd* 1996;**240**:193–9.
25. Kaneyoshi T, Takahashi T, Hayashi Y, Motoyama M. Preparation of Al_3Nb and Al_3Nb–NbC composite by mechanical alloying. In: *Proceedings of the proceedings of the 1992 powder metallurgy world congress. Part 1 (of 9)*. 1992. p. 421–9.
26. Kaneyoshi T, Takahashi T, Motoyama M. Reaction of niobium with hexane and methanol by mechanical grinding. *Scripta Metall Mater* 1993;**29**:1547–51.
27. Yelsukov EP, Barinov VA, Ovetchkin LV. Synthesis of disordered Fe_3C alloy by mechanical alloying of iron powder with liquid hydrocarbon (toluene). *J Mater Sci Lett* 1992;**11**:662–3.
28. Zhang W, Li Z, Zhang D. Synthesizing AlN powder by mechanochemical reaction between aluminum and melamine. *J Mater Res* 2010;**25**:467–70.
29. Zhang F, Kaczmarek WA, Lu L, Lai MO. Formation of titanium nitrides via wet reaction ball milling. *J Alloys Compd* 2000;**307**:249–53.
30. Sun JF, Wang MZ, Zhao YC, Li XP, Liang BY. Synthesis of titanium nitride powders by reactive ball milling of titanium and urea. *J Alloys Compd* 2009;**482**:L29–31.
31. Wang GM, Campbell SJ, Kaczmarek WA. Mechanochemical nitridation by ball milling iron with pyrazole: a structural investigation. *Mater Sci Eng A* 1997;**226–228**:80–3.
32. Kaczmarek WA. Crystallographic and magnetic properties of fine iron nitride powders prepared by solid state reactions between iron and organic H_x(CN)-ring compounds. *Scripta Metall Mater* 1995;**33**:1687–94.
33. Keskinen J, Pogany A, Rubin J, Ruuskanen P. Carbide and hydride formation during mechanical alloying of titanium and aluminum with hexane. *Mater Sci Eng A* 1995;**196**:205–11.
34. Niu XP, Froyen L, Delaey L, Peytour C. Hydride formation in mechanically alloyed Al–Zr and Al–Fe–Zr. *Scripta Metall Mater* 1994;**30**:13–8.
35. Tokumitsu K. Formation of metal hydride powders and metal-hydrogen amorphous powders by mechanochemical reaction. *J Less-Common Met* 1991;**172**:153–9.
36. Suzuki TS, Nagumo M. Metastable intermediate phase formation at reaction milling of titanium and n-heptane. *Scripta Metall Mater* 1995;**32**:1215–20.
37. Nagumo M, Suzuki TS, Tsuchida K. Metastable states during reaction milling of hcp transition metals with hydrocarbon. *Mater Sci Forum* 1996;**225–227**:581–6.
38. Williamson GK, Hall WH. X-ray line broadening from filed aluminium and wolfram. *Acta Metall* 1953;**1**:22–31.
39. Lutterotti L, Matthies S, Wenk HR. MAUD: a friendly Java program for material analysis using diffraction. *IUCr: Newsl of the CPD* 1999;**21**:2.
40. Typical values obtained for the *sig.* (profile factor) and Rwp (weighted profile factor) is 1.95 and 0.15, respectively.
41. Manna I, Chattopadhyay PP, Banhart F, Fecht HJ. Formation of face-centered-cubic zirconium by mechanical attrition. *Appl Phys Lett* 2002;**81**:4136–8.
42. Aigner K, Lengauer W, Rafaja D, Ettmayer P. Lattice-parameters and thermal-expansion of $Ti(C_xN_{1-x})$, $Zr(C_xN_{1-x})$, $Hf(C_xN_{1-x})$ and TiN_{1-x} FROM 298-K to 1473-K as investigated by high-temperature X-ray-diffraction. *J Alloys Compd* 1994;**215**:121–6.
43. Fredrickson DR, Hubbard WN, Nuttall RL, Flotow HE. Enthalpies of formation of zirconium dihydride and zirconium dideuteride. *J Phys Chem* 1963;**67**:1506–9.
44. Baker FB, Storms EK, Holley CE. Enthalpy of formation of zirconium carbide. *J Chem Eng Data* 1969;**14**:244–6.
45. Borchers C, Leonov AV, Morozova OS. Mechanical activation of structural and chemical transformations in a Zr–C–H system in two stages. *J Phys Chem B* 2002;**106**:1843–8.
46. Chen Y, Williams JS. Competitive gas–solid reactions realized by ball milling of Zr in ammonia gas. *J Mater Res* 1996;**11**:1500–6.